Available online at www.sciencedirect.com
ScienceDirect
Journal of Power Sources 159 (2006) 49–54
JOURNAL OF POWER SOURCES
www.elsevier.com/locate/jpowsour

Short communication

Deposition of ZrO_2 film by liquid phase deposition

Jain-Ming Lin, Ming-chi Hsu, Kuan-Zong Fung *

Department of Materials Science and Engineering, National Cheng Kung University, Tinan 70101, Taiwan

Available online 11 July 2006

Abstract

In this study, undoped ZrO_2 thin films were deposited on single-crystal silicon substrates using liquid phase deposition. The undoped films were formed by hydrolysis of zirconium sulfate ($Zr(SO_4)_2{\cdot}4H_2O$) in the presence of H_2O. A continuous oxide film was obtained by controlling adequate $(NH_4)_2S_2O_8$ concentration. The deposited films were characterized by SEM, FT-IR, XRD and DTA. Typically, the films showed excellent adhesion to the substrate with uniform particle diameter about 150 nm. The thicknesses of ZrO_2 film were about 200 nm after 10 h deposition at 30 °C. These films shows single tetragonal phase after heat treated at 600 °C. High annealing temperature (e.g. 750 °C) may result in the phase transformation of (t)-ZrO_2 into (m)-ZrO_2.

Keywords: Thin film; ZrO_2; Liquid phase deposition

1. Introduction

Due to the excellent thermal, mechanical stability, and electrical properties of zirconia, thin film processing of zirconia plays an important role for optical, dielectric, corrosion-resistant coatings, and sensor applications. Moreover, the application of ZrO_2 film has been focused on high-temperature electrochemical devices, such as solid electrolyte in solid oxide fuel cells (SOFCs). In the solid electrochemical applications using YSZ thin film, the process of tape casting or colloidal deposition combined with high temperature sintering (∼1400 °C) is fairly common. When the YSZ thin film is obtained from the sintering of fine powder, the reaction with the substrate is inevitable. Such a reaction may degrade the performance of the electrochemical devices. Thus, the synthesis of a dense YSZ thin film at low temperature is very much desirable. For instance, when a thin film of YSZ is able to deposit on the substrate of LSM cathode substrate for SOFC applications, the formation of $LaZrO_3$ can be avoided.

Two kinds of low-temperature wet-chemical methods, the self-assembled monolayer (SAM) technique [1–5] and the liquid-phase deposition (LPD) [6–9], have been recently developed for direct deposition of ZrO_2 thin films using aqueous solutions. Agarwal et al. [1] first studied the deposition of ZrO_2 thin film on a SAM surface using hydrolysis of zirconium sulfate ($Zr(SO_4)_2{\cdot}4H_2O$) in HCl (pH < 1) solution at 70 °C. The dense and well-adhered ZrO_2 films with tetragonal phase could be obtained as the film calcined at 500 °C for 2 h. Polli et al. [5] also prepared nanocrystalline zirconia film via SAM method from an aqueous dispersion without visible bulk precipitation. In SAM process, SAM polymer is deposited by immersing the substrate in organic solution of the hydrocarbon, $X–(CH_2)_n–Z$, where X denotes the "surface group," chosen sulfonate ($–SO_3H$). The sulfonate group is very effective in initiating and sustaining the formation of oxide thin films. Therefore, the thickness of oxide film may be restricted by sulfonate group surface condition (e.g. uniformity, and adhesion).

The LPD [6–9], on the other hand, is a very simple and inexpensive method without the need of special equipment such as vacuum system. A soluble hydride hexafluorozirconate (H_2ZrF_6) easily hydrolyzes in an aqueous solution by the release of fluorine ions, and subsequently reacts with boric acid. Hence, the hydrolysis reactions proceed and the ZrO_2 deposits forms on the substrate. However, it is difficult to remove the residual fluorine in the as-prepared thin film. To obtain ZrO_2 film by LPD method, the starting reagent other than H_2ZrF_6 is needed. Therefore, the main objective of this work is to find a novel method to obtain ZrO_2 thin film at temperature lower than 1000 °C. The starting materials used were zirconium sulfate ($Zr(SO_4)_2{\cdot}4H_2O$), and ammonium persulfate ($(NH_4)_2S_2O_8$). The effect of persulfate concentration was investigated. Such a low-temperature thin film process will be beneficial to the

* Corresponding author. Tel.: +886 6 275 7575; fax: +886 6 238 0208.
E-mail address: kzfung@mail.ncku.edu.tw (K.-Z. Fung).

0378-7753/$ – see front matter © 2006 Elsevier B.V. All rights reserved.
doi:10.1016/j.jpowsour.2006.04.116

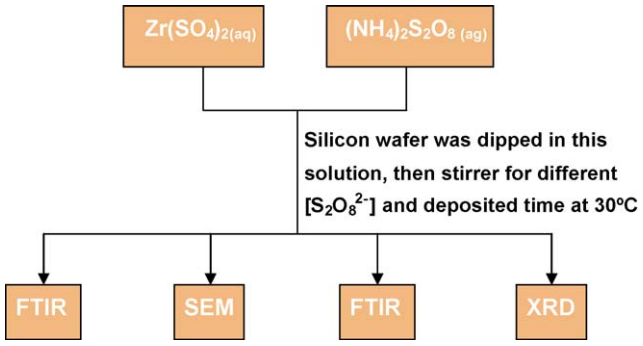

Fig. 1. Schematic flowchart for the solution preparation and film deposition.

formation of thin zirconia electrolyte in order to eliminate the reaction between cathode and electrolyte.

2. Experimental procedure

2.1. Films preparation

The experimental flowchart is shown in Fig. 1. Zirconium sulfate ($Zr(SO_4)_2{\cdot}4H_2O$, 98+%, Alfa Aesor), and ammonium persulfate ($(NH_4)_2S_2O_8$, 98%, Riedel-de Haën) were first dissolved in deionized water at 30 °C. A mixture of $Zr(SO_4)_2{\cdot}4H_2O$ and $(NH_4)_2S_2O_8$ with $Zr^{4+}/S_2O_8{}^{2-}$ ratio varying from 0.2 to 1 was used as the starting solution. After the mixture was stirred for 5 min, a homogenous clean solution was obtained. The substrate of 2 cm × 2 cm silicon wafer was cleaned sequentially in organic solvents (acetone and isopropyl alcohol) and oxidizing Piranha solution (mixture of 70% H_2SO_4:30% H_2O_2) at 80 °C. Then, the cleaned substrates were immersed into the prepared solution at 30 °C on a stirring plate to deposit a thin film. After immersion for 1, 3, 5, 10, 15, and 20 h, the substrates were rinsed three times in deionized water, and cleaned ultrasonically for 30 min. Some films were heated at to 500, 600, 650, 700, and 750 °C a heating rate of 5 °C min^{-1} in air, respectively.

2.2. Characterization of deposition film

The morphology and thickness of the ZrO_2 film was examined by scanning electron microscope (SEM, Hitachi S4100). The crystal structure of thin films were characterized by using X-ray diffraction (XRD, Rigaku ATX-E). XRD was performed using an X-ray diffractometer with Cu Kα radiation and Ni filter operated at 30 KV, 20 mA and a scanning rate of 1° min^{-1}.

Differential thermal and themogravimetric analyses (DTA/TGA) were conducted on a powder sample at a heating rate of 5 °C min^{-1} in air with Al_2O_3 powder as a reference.

The precipitated powder in solution was filtered and analyzed by Fourier transform infrared (FT-IR, Perkin-Elmer spectrum one) spectroscopy with KBr as reference.

3. Results and discussion

3.1. The film deposition mechanism

In previous study [10], the aqueous $Zr(SO_4)_2{\cdot}4H_2O$ solution was a metastable supersaturated solution. The precipitation of zirconium compound occurred spontaneously. The precipitation rate increased with decreasing $Zr(SO_4)_2{\cdot}4H_2O$ aqueous concentration. In present process, $S_2O_8{}^{2-}$ was added into this supersaturated solution in order to suppress the formation of zirconium precipitates from homogenous nucleation in solution. Consequently, the initiating film deposited on the functionalized silicon surface via heterogeneous nucleation. The SEM micrographs of deposited oxide films from different $[S_2O_8{}^{2-}]$ are shown in Fig. 2. The SEM micrographs of the same films heat-treated at 750 °C for 3 h are also shown in Fig. 3. When $[S_2O_8{}^{2-}]$ was as low as 0.005 M, numerous large particles (diameter = 150 nm) were clearly observed. It suggests that the precipitation of $7ZrO_2{\cdot}5SO_3{\cdot}30H_2O_{(s)}$ particles in dilute $[S_2O_8{}^{2-}]$ was faster than high $[S_2O_8{}^{2-}]$. The $7ZrO_2{\cdot}5SO_3{\cdot}30H_2O_{(s)}$ particles were easily deposited on substrate, and grown into large particles. On the contrary, at $Zr(SO_4)_2{\cdot}4H_2O$ aqueous solution with high $[S_2O_8{}^{2-}]$, the small $7ZrO_2{\cdot}5SO_3{\cdot}30H_2O_{(s)}$ particles nucleated more homogenously and formed small particles. The small particles were not easily to grow into large particles. Among the large particles, the continuous and dense as-deposited film was formed. From these results we may suggest that the $S_2O_8{}^{2-}$ ions would effectively suppress the formation of zirconium precipitation, and improve the initiating film growing via heterogeneous nucleation on silicon wafer.

The following chemical reactions [11] show that the dissolution of zirconium sulfate in water and the formation of supersaturated solution. At least two processes occur simultaneously in these solutions: the formation of sulfate complexes (1) and hydrolysis (2):

$$7Zr(SO_4)_2 + 2H_2O \rightarrow 7ZrOSO_4{\cdot}5SO_3 + 2H_2SO_4 \quad (1)$$

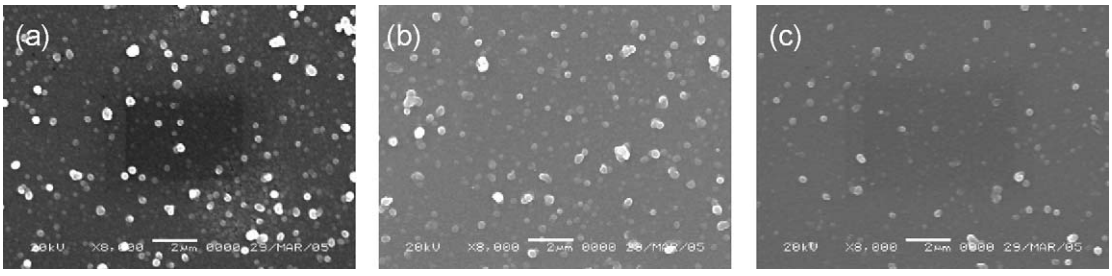

Fig. 2. The SEM image of as-deposited ZrO_2 films prepared from different $[S_2O_8{}^{2-}]$ concentration: (a) 0.005 M, (b) 0.015 M, and (c) 0.025 M. The deposition time was 3 h.

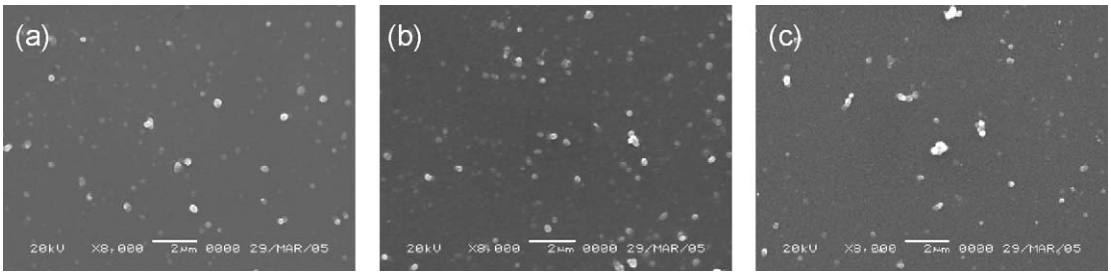

Fig. 3. The SEM image of ZrO_2 films prepared from different [$S_2O_8^{2-}$] concentration: (a) 0.005 M, (b) 0.015 M, and (c) 0.025 M after 2 h annealing at 750 °C in air. The deposition time was 3 h.

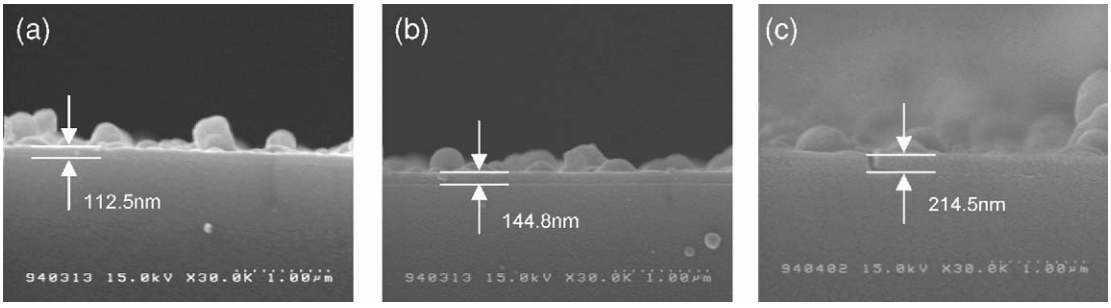

Fig. 4. The SEM image of zirconia thin film showing different thickness under various deposition time: (a) 3 h, (b) 5 h, and (c) 20 h when 0.005 M $Zr(SO_4)_{2(aq)}$ and 0.015 M $(NH_4)_2S_2O_{8(aq)}$ were used.

$$7ZrSO_4{\cdot}5SO_3 + 37H_2O \rightarrow 7ZrO_2{\cdot}5SO_3{\cdot}30H_2O(\text{amorphous}) + 7H_2SO_4 \quad (2)$$

However, $S_2O_8^{2-}$ ion is a strong oxidizing agent. When $(NH_4)_2S_2O_8$ dissolved in water, the following two reactions occur:

$$2H_2O \rightarrow O_2 + 4e^- + 4H^+ \quad (3)$$

$$2S_2O_8^{2-} + 4e^- \rightarrow 4SO_4^{2-} \quad (4)$$

Reaction (3) causes the release of O_2 from water; reaction (4) is the reduction of $S_2O_8^{2-}$ into SO_4^{2-}. Reactions (3) and (4) may be used to control [H_2SO_4] in the precursor solution. Subsequently, the formation of $7ZrO_2{\cdot}5SO_3{\cdot}30H_2O_{(s)}$ may be effectively controlled based on reaction (2). Finally, a continuous film may form through heterogeneous nucleation on the silicon surface.

3.2. The film thickness

The cross-sectional SEM image of the deposited thin films before and after annealing at 750 °C are shown in Figs. 4 and 5. The thickness increased with deposition time. The growth of ZrO_2 seems to follow a nucleation process.

Especially, the oxide film after 750 °C annealing showed columnar morphology (Fig. 5) Cross-sectional observation also suggested that the thickness of the deposited film, decreased from 144.8 nm (Fig. 4b) to 123.2 nm after annealing (Fig. 5b), representing a shrinkage of about 15%. This film shrinkage may result from the decomposition of unstable components such as H_2O, hydroxyl groups, amino group, and oxysulfide as detected by FT-IR.

The film thickness measured by using scanning electron microscope was plotted as a function of the deposition time. A non-linear dependence of ZrO_2 film thickness against deposition time for different [Zr^{2+}]/[$S_2O_8^{2-}$] ratio is shown in Fig. 6. Subsequently, different $(NH_4)_2S_2O_8$ concentrations, namely 0.005,

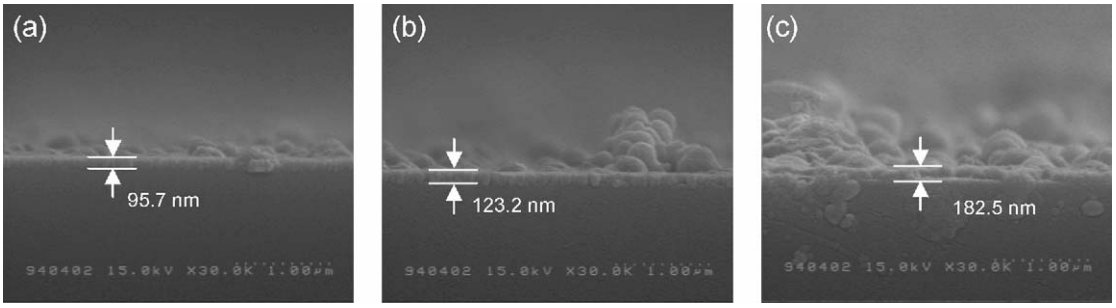

Fig. 5. SEM image of zirconia thin film after 750 °C heat-treatment showing different thickness under various deposition time (a) 3 h, (b) 5 h, and (c) 20 h when 0.005 M $Zr(SO_4)_{2(aq)}$ and 0.015 M $(NH_4)_2S_2O_{8(aq)}$ were used.

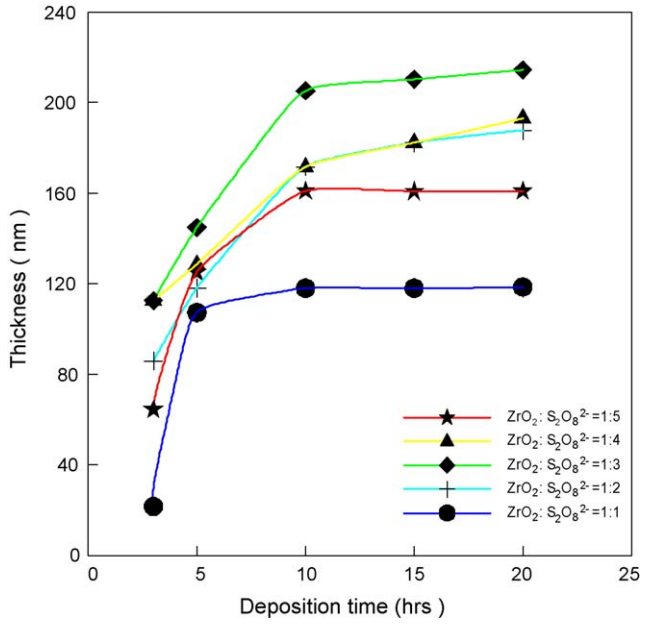

Fig. 6. Thickness of ZrO_2 plotted as a function of deposition time using various $[Zr^{2+}]/[S_2O_8{}^{2-}]$ ratio.

0.01, 0.015, 0.02, and 0.025 M were added, and the deposition time extended to 20 h. All curves started with an oblique line, the ZrO_2 thin film thickness increased with increasing deposition time. After 10 h, the thickness of ZrO_2 was levelled. This result suggests that the chemical reaction in solution already reached dynamic equilibrium. When $[Zr^{4+}]/[S_2O_8{}^{2-}]$ was 0.005/0.015, the ZrO_2 film thickness reached 174.6 nm during 10 h deposition. The growth rate of ZrO_2 film was estimated to be about 11.2 nm h^{-1}. Fig. 7 shows the ZrO_2 film grow rate (between 3 and 10 h) versus $S_2O_8{}^{2-}$ ion concentration. From this figure it was clear to reveal $S_2O_8{}^{2-}$ being an inhibitor in the precursor solution. The growth rate of film decreased with increasing $[S_2O_8{}^{2-}]$. Specially, when $[S_2O_8{}^{2-}]$ reached 0.02 M, the growth rate of ZrO_2 film was down to 9.29 nm h^{-1} because higher $[S_2O_8{}^{2-}]$ tends to shift reaction (2) toward the left hand side.

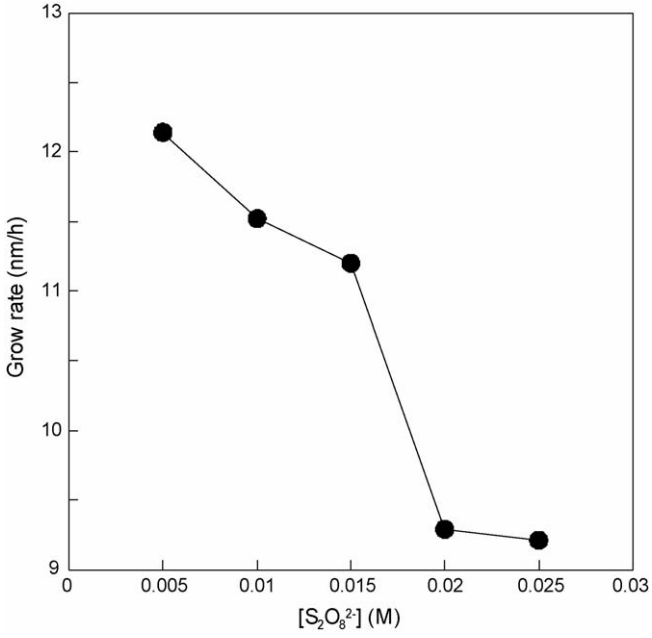

Fig. 7. Growth rate of ZrO_2 film vs. different $S_2O_8{}^{2-}$ concentration.

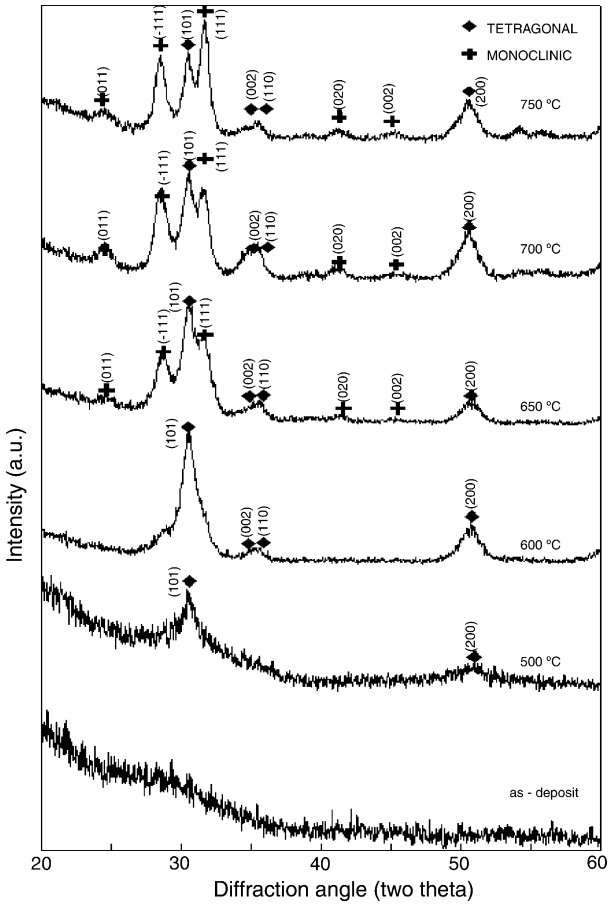

Fig. 8. The XRD profiles taken from deposited films after heat-treated at various temperatures.

3.3. XRD analysis

Fig. 8 shows the XRD profiles for the as-deposited thin film and those after annealed at different temperatures for 2 h in air. The as-deposited film was amorphous, and no obvious diffraction peaks were detected. After annealing at 600 °C, diffraction peaks appearing at 30.5°, 34.8°, 35.3°, and 50.7° correspond to (1 0 1), (0 0 2), (1 1 0), and (2 0 0) plane of tetragonal phase ZrO_2 (t-ZrO_2). After the film was annealed at 650 °C, a new phase, monoclinic ZrO_2 (m-ZrO_2), was observed, accompanying the decrease in intensity of (1 0 1) diffraction of t-ZrO_2.

This phase transformation has also been observed in ZrO_2 films grown through other chemical solution routes [1–4,9,12–14]. The formation of metastable t-ZrO_2 phase, versus the thermodynamically stable monoclinic phase at such low temperatures has been attributed to the fine crystallite size [15] of ZrO_2 from the amorphous phase. The small crystallite tends to enhance the stability of t-ZrO_2, due to the volume change associated with the (t)-ZrO_2 → (m)-ZrO_2 transformation.

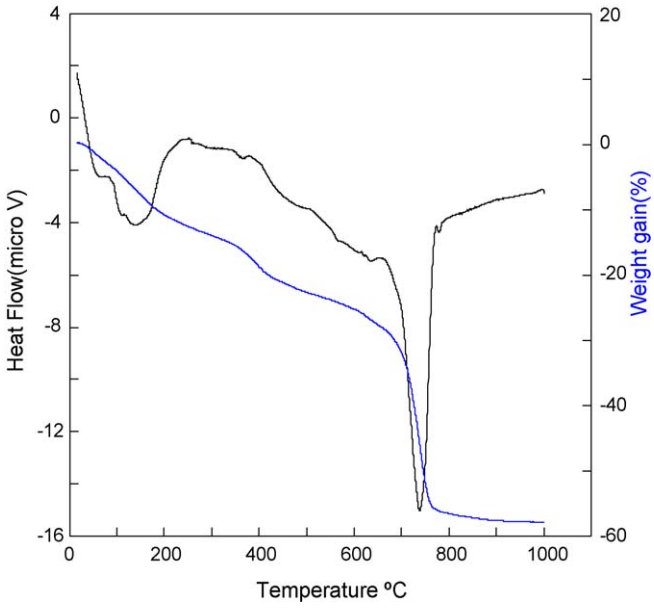

Fig. 9. TG-DTA curves for the as-deposited precipitate.

3.4. DTA and FT-IR analyses

The DTA curve (Fig. 9) of the precipitate formed after 20 h in the solution revealed three weight loss at 200, 500, and 750 °C. Under 200 °C, the weight loss was due to the evaporation of absorbed water. From FT-IR analysis, the weight loss about 9.2% at 500 °C is associated with NH_4^+ and some OH group. The NH_4^+ band was completely removed at 500 °C. The noticeable weight loss about 57% and exothermic reactions occurred at 750 °C. Such a reaction was attributed to the formation of ZrO_2 from the removal of metastable chemical band SO_2–OH group, and SO_3 group.

Fig. 10 shows the FT-IR spectrum of the precipitate collected after deposition. The 1640 cm^{-1} band is assigned to the OH stretching. The 1236 cm^{-1} band is assigned to the NH_4^+ group, that was completely removed at 500 °C. The appearance of SO_2–OH band at 2300 cm^{-1} was a metastable chemical band, when the as-deposited sulfate complexes was annealed at 300, and 500 °C. The band at 1000–1239 cm^{-1} assigned to SO_3–H_2O stretching, and SO_3 band resulted from SO_3–H_2O stretching above 200 °C. The absorbed water was removed above 200 °C. The amorphous Zr–O bands were located at 847, 640, 499 cm^{-1}. When this powder was annealed at 500 °C, the band at 847 cm^{-1} intensified. This result suggests that ZrO_2 film started to crystallize, and the Zr–O band strength became strong at 847 cm^{-1}. Further heating at 750 °C removed the sulfur signal disappeared completely. The Zr–O band also transferred to crystalline ZrO_2 bands located at 748, 667, 583 and 503 cm^{-1}.

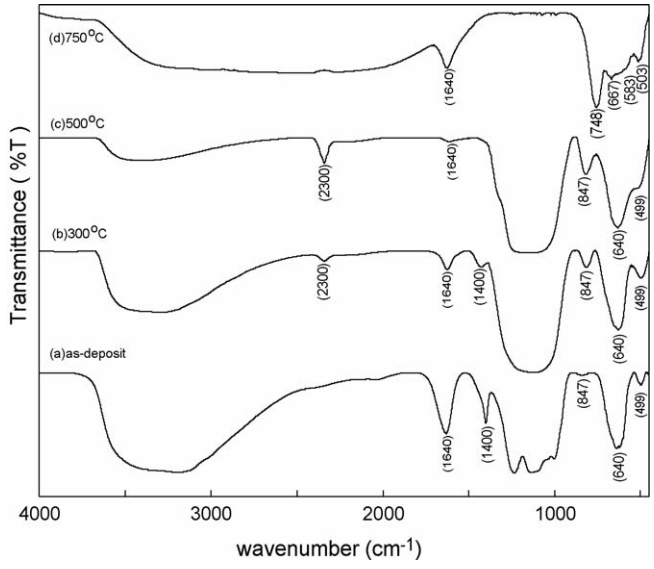

Fig. 10. FT-IR spectra for the as-prepared powder and those after annealing at different temperatures.

From the DTA and FT-IR results, the as-deposited film consisted of SO_3–H_2O, NH_4^+, OH group, and amorphous Zr–O band. Around 200 °C, the absorbed water was evaporated, and the SO_3–H_2O decomposed to SO_3 and SO_2–OH band. At 500 °C, the OH group and NH_4^+ band were completely removed, and the amorphous Zr–O band also transfer to crystalline ZrO_2 band. After 750 °C annealing, the SO_3 and SO_2–OH bands were removed completely. Above 750 °C annealing, the ZrO_2 thin film was obtained without the presence of impurities.

4. Conclusions

A novel method for preparing zirconium-complex aqueous solution using simple inorganic substances such as zirconium sulfate ($Zr(SO_4)_2{\cdot}4H_2O$), and ammonium persulfate ($(NH_4)_2S_2O_8$) was established:

(1) Amorphous, homogenous, and well-adhered ZrO_2 was obtained from zirconium sulfate ($Zr(SO_4)_2{\cdot}4H_2O$), and ammonium persulfate ($(NH_4)_2S_2O_8$) precursor solution.
(2) After annealing, the metastable tetragonal phase ZrO_2 thin film was observed at 550 °C. Above 600 °C the coexistence tetragonal and monoclinic phase ZrO_2 was observed form XRD analysis.
(3) During heating, the NH_4^+ band was removed at 500 °C, and metastable band like SO_2–OH group, and SO_3–H_2O group was eliminated at 750 °C based on the results of FT-IR and DTA.

Acknowledgement

This work is financially supported by National Science Council (NSC) in Taiwan under the grant no. NSC 93-2120-M-006-004.

References

[1] M. Agarwal, M.R. De Guire, A.H. Heuer, J. Am. Ceram. Soc. 80 (1997) 2967–2981.
[2] Y.F. Gao, Y. Masuda, T. Yonezawa, K. Koumoto, J. Ceram. Soc. Jpn. 110 (2002) 379–385.
[3] T.P. Niesen, M.R. De Guire, J. Bill, F. Aldinger, M. Rühle, A. Fischer, F. Jentoft, Schlögl, J. Mater. Res. 14 (1999) 2464–2475.
[4] H. Shin, M. Agarwal, M.R. De Guire, Acta Mater. 46 (1998) 801–815.

[5] A.D. Poli, T. Wagner, A. Fischer, G. Weinberg, F.C. Jentoft, R. Schlögl, M. Rühle, Thin Solid Films 379 (2000) 122–127.
[6] T. Yao, T. Inui, A. Ariyoshi, J. Am. Ceram. Soc. 79 (1996) 3329–3330.
[7] T. Yao, J. Mater. Res. 13 (1998) 1091–1098.
[8] N. Ozawa, T. Yao, Trans. Mater. Res. Soc. Jpn. 28 (2003) 321–330.
[9] G. Yanfeng, M. Yoshitake, H. Masuda, K. Kunihito, Chem. Mater. 16 (2004) 2615–2622.
[10] M. Windholz, N.J. Rahway, (Eds.), The Merck Index, 10th ed., Mereck & Co., Inc., 1983, p. 1460.
[11] E. Pietsch et al. (Eds.), Gmelin's Handbuch der Anorganischen Chemie, Verlag Chemie, 1926.
[12] I. Zhitomirsky, L. Gal-Or, A. Kohn, H.W. Hennicke, J. Mater. Sci. 30 (1995) 5307–5311.
[13] R. Chaim, I. Silberman, L. Gal-Or, J. Electrochem. Soc. 138 (1991) 1943–1947.
[14] R. Chaim, G. Stark, L. Gal-Or, H.J. Bestgen, Mater. Sci. 29 (1994) 6241–6244.
[15] R.C. Garvie, J. Phys. Chem. 69 (1965) 1238–1243.